



High temperature oxidation of nickel-based alloys reinforced by hafnium carbides. Part 1 : Thermogravimetry results

Elodie Conrath, Patrice Berthod*

Institut Jean Lamour (UMR 7198), Team 206 "Surface and Interface, Chemical Reactivity of Materials"
University of Lorraine, Faculty of Sciences and Technologies, B.P. 70239, 54506 Vandoeuvre-lès-Nancy, (FRANCE)
E-mail: Patrice.Berthod@univ-lorraine.fr

ABSTRACT

Hafnium, element known to be especially active in oxidation at high temperature, was added in high quantities to model chromium-rich carbon-containing nickel-based alloys, in order to promote the formation of hafnium carbides preferentially to chromium carbides. As earlier seen for cobalt-based alloys displaying such hafnium contents, hafnium effectively favoured the formation of interdendritic HfC carbides and then led to special nickel-based alloys the behaviour in oxidation at high temperature of which was then studied. This was done in artificial dry air at 1200°C during 46 hours after a heating phase and before a cooling phase which were both also characterized: in terms of temperature start and thereafter rate of oxidation during heating, and of oxide spallation temperature start and amplitude of mass loss during cooling. Some of the obtained results were conform with what was observed for Hf-free and Hf-containing cobalt-based alloys for almost the same oxidation cycle, such as lower temperatures of oxidation start at heating and of oxide spallation at cooling, but differences were also noticed and are here described.

© 2013 Trade Science Inc. - INDIA

KEYWORDS

Nickel-based alloys;
Hafnium carbides;
Transient oxidation;
High temperature oxidation;
Oxide spallation.

INTRODUCTION

Many high temperature applications require especially high mechanical properties of the used materials such as creep-resistance^[1]. The most efficient nickel-based superalloys for such use are actually the γ/γ' single crystal ones, the microstructure^[2] of which provide very high strength for service temperature near 1000°C and slightly above, which is sufficient even for working at higher temperatures since, for instance, the hottest turbine blades are internally air-cooled.

These γ/γ' nickel-based superalloys are also extremely oxidation-resistant in air thanks to their alumina-forming behaviour^[3] but they are unfortunately not suitable for glass-working for example, or for other situations where corrosion by molten substances may act and require the presence of several tens of weight percents of chromium^[4,5]. Unfortunately nickel-based alloys containing chromium enough to resist high temperature corrosion cannot be reinforced by gamma prime precipitates and other strengthening phases must be used instead. Carbides are among the most com-

mon reinforcing particles in cast superalloys, whatever the base, cobalt or nickel. The presence of twenty or thirty weight percents of chromium is favourable for the development of primary chromium carbides but these ones are usually not stable enough at temperatures especially high (1200°C for example) and other types of carbides must be obtained. This may be achieved by adding sufficiently high amounts of strong MC-forming elements but some of these carbides, TaC for example, may encounter difficulties to stay in chromium-rich nickel-based alloys at high temperature and even before to precipitate during solidification^[6]. In contrast, hafnium, which is also a strong former of MC carbides, was recently successfully used to obtain a significant population of MC carbides in 25 wt.%Cr-containing nickel-based alloys^[7] in which HfC carbides formed preferentially to chromium carbides. Since Hf is not only an especially strong carbides-forming element but also a very active element in the high temperature oxidation point of view, it appeared important to test the behaviour in oxidation at high temperature of nickel-based alloys reinforced by HfC carbides.

Thus, in the present work, the three alloys Ni-25Cr-xC-yHf, earlier elaborated and the as-cast microstructure and hardness of which were specified^[7], were exposed in hot air during more than forty hours at 1200°C – level of temperature at which HfC-reinforced nickel-based alloys can be of great interest by comparison with nickel alloys simply strengthened by chromium carbides – in order to observe their behaviour during heating and cooling as well as in isothermal condition, as this was done for similar HfC-containing cobalt alloys in a previous work^[8].

EXPERIMENTAL DETAILS

The alloys of the study

The three HfC-strengthened nickel-based alloys, the as-cast microstructures of which were already described^[7] were synthesized by High Frequency Induction melting from pure elements (Ni, Cr, Hf and C) in a chamber filled by 300mbar of argon. Their solidification was achieved in the water-cooled copper crucible of the used HF furnace, which led to 40g-weighing in-

gots. Their “{targeted composition}-names” and the chemical compositions which were obtained (measured by the Energy Dispersive Spectrometry device equipping the SEM JEOL JSM-6010LA) were:

- (1) “Ni-25Cr-0.25C-3.72Hf”: 25.70wt.% Cr and 4.40wt.% Hf (Co: bal., C: not measured)
- (2) “Ni-25Cr-0.50C-3.72Hf”: 25.57wt.% Cr and 4.79wt.% Hf (Co: bal., C: not measured)
- (3) “Ni-25Cr-0.50C-5.58Hf”: 25.32wt.% Cr and 6.64wt.% Hf (Co: bal., C: not measured)

Here too, four Ni-25wt.%C-xC (with x=0, 0.25, 0.50, and 1.00wt.%) alloys were also elaborated in parallel with the same elaboration for comparing the hardness values between the Hf-containing and the Hf-free alloys. Only two of these four alloys, the ones having the same targeted contents in carbon as the studied Hf-containing alloys, were considered for comparison:

- (1) “Ni-25Cr-0.25C”: 23.79wt.% Cr (Co: bal., C: not measured)
- (2) “Ni-25Cr-0.50C”: 22.74wt.% Cr (Co: bal., C: not measured)

Preparation of the samples for the thermogravimetry tests

Similarly to the cobalt-based alloys of the first part of this work, the five ingots were cut near the centre of the ingot to obtain almost parallelepipedic samples, by avoiding the most external zone where pro-eutectic HfC carbides segregated and to ensure a chemical and microstructural homogeneity. These samples were grinded with 240-grade SiC papers to smooth edges and corners, before being wholly polished with 1200-grade ones (main faces notably). A Setaram TG92 thermobalance was used for the thermogravimetry runs, which were performed in dry artificial air (80%N₂-20%O₂). Globally, except the isothermal stage duration, the same thermal cycle as for the cobalt-based alloys^[8] was applied: heating at 20°C min⁻¹, the isothermal (1200°C) stage duration of 46 hours (except 50 hours for the cobalt-based alloys), and the cooling at -5°C min⁻¹. Here too the exploitations of the mass gain files for the heating part and for the cooling part were done following the same procedures as for the cobalt-based alloys of the first part^[9,10].

Full Paper

RESULTS AND DISCUSSION

Initial microstructures of the alloys

It can be reminded that the microstructures of the three Hf-containing nickel-based alloys all displays an austenitic dendritic matrix of nickel-based solid solution and exclusively hafnium carbides, except the second alloy for which there are more atoms carbon than hafnium carbon which permitted obtaining also chromium carbides (example of its microstructure given in Figure 1).

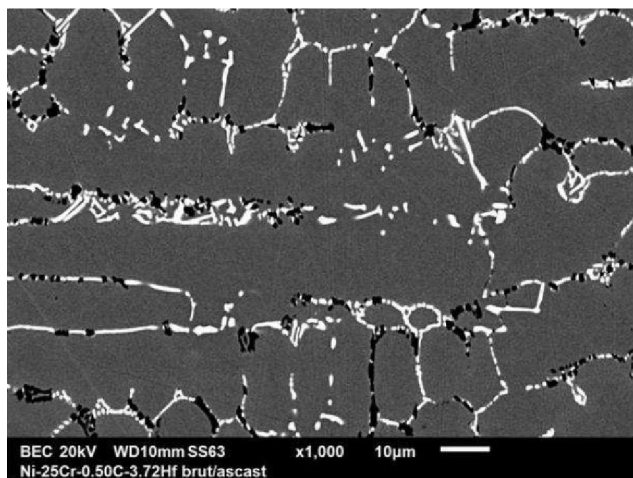


Figure 1 : Example of as-cast microstructure of a HfC-strengthened alloy (here: Ni-25Cr-0.50C-3.72Hf alloy)

Almost all HfC carbides are eutectic “script-like” shaped and they are present in the interdendritic areas where there are mixed with the austenitic matrix. It is however true that other HfC carbides, blocky and having all segregated to the exterior domain of the ingot, are also present. But no of these HfC carbides – probably pro-eutectic carbides – stayed in the centre of the ingots, in contrast with the cobalt-based alloys for which the pro-eutectic carbides were seemingly much more present, in the ingots’ centers as well as in their peripheries. The carbide densities were logically higher for higher carbon and/or hafnium content(s), as is to say for the Ni-25Cr-0.50C-5.58Hf and Ni-25Cr-0.50C-3.72Hf alloys than for the Ni-25Cr-0.25C-3.72Hf one.

Exploitation of the obtained mass gain curves

The thermogravimetry results were plotted by representing the mass gain versus temperature in order to study more easily what occurred during heating as well

as during cooling (examples displayed in Figure 2). All the obtained mass gain curves were studied first in their heating part to assess the temperature at which oxidation began (with a consecutive mass gain. As for the cobalt-based alloys of the first part of this work the mass curves were preliminarily corrected from the air buoyancy variations.

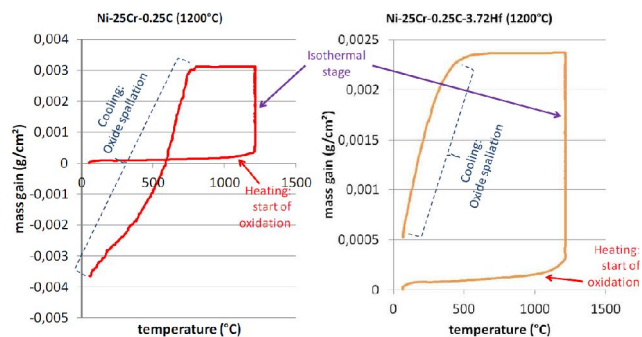


Figure 2 : Two examples illustrating the plotting of mass gain curves versus temperature instead versus time (and evidencing the effect of hafnium on oxide spallation during cooling)

Results: Oxidation at heating

The first results given by these kinds of data treatment (correction from air buoyancy variations) and plot ($\Delta m/S = f(T)$ instead $f(t)$) were the temperature at which oxidation has become fast enough to induce mass gain high enough allowing its detection by the thermobalance. These oxidation start temperatures determined for the five alloys are presented together graphically in Figure 3. This histogram shows that oxidation began to be detectable with the used thermobalance after more time of heating in the case of the two Hf-free alloys than for the three Hf-containing ones. This is especially true for the two Hf-containing alloys also containing 0.50 wt.%C for which the mass gain by oxidation was detected at around 750°C, as is to say more than 100°C under the other alloys.

This can be compared with what was found for the corresponding cobalt-based alloys studied in the first part of this work^[8]: if the oxidation start temperatures (o.s.t.) of the Hf-free nickel-based alloys are of the same level as for the previously studied Hf-free cobalt-based alloys, the o.s.t. of the Hf-containing Ni-based alloys are lower than for the Hf-containing Co-based alloys, especially for the two 0.50wt.%C ones (between 130 and 150°C lower).

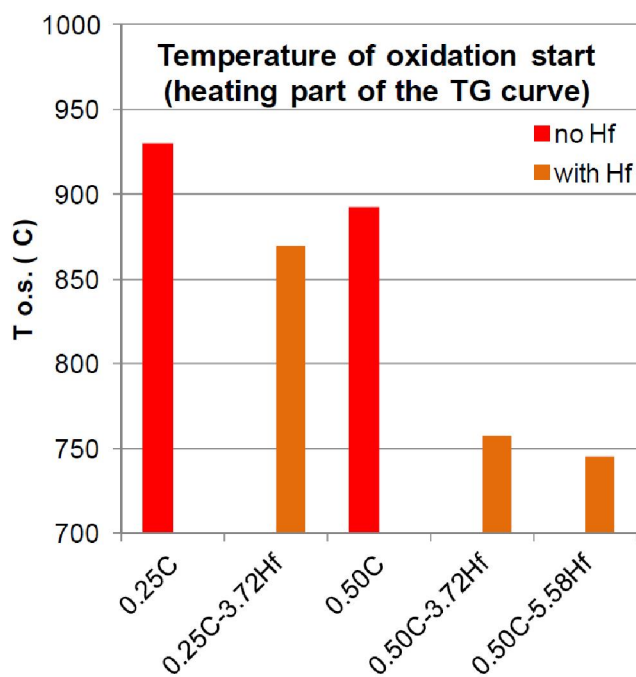


Figure 3 : Temperatures at which the mass gain due to real oxidation became detectable by the thermo-balance during the heating, for each of the five alloys (Ni-25wt.%Cr-xC(-yHf))

The total mass gain obtained during the whole heating were determined on the same heating parts of these ($\Delta m/S = f(T)$) curves are presented, as histogram too, in Figure 4. It can be seen that these mass gains achieved between the oxidation detection and the beginning of the isothermal dwell tend to be lower in presence of Hf for the alloys containing 0.25wt.%C and inversely higher in presence of Hf for the alloys containing 0.50wt.%C. One can notice that the evolution of this mass gain at heating seems decreasing for the Hf-free nickel-based alloys and in contrast increasing for the Hf-containing ones, when the carbon content increases. When these results are compared with their analogous ones previously obtained for the corresponding cobalt-based alloys it appears first that the effect of Hf is inverse (Hf led to lower mass gains at heating for the Co-based alloys) and second the mass gains are seemingly the same for the Ni-based alloys and for the Co-based ones when Hf is present while, in contrast, the mass gains at heating were much higher for the Hf-free Co-based alloys than for the Hf-free Ni-based ones (which explains the inversion of the effect of Hf between the two bases of alloys).

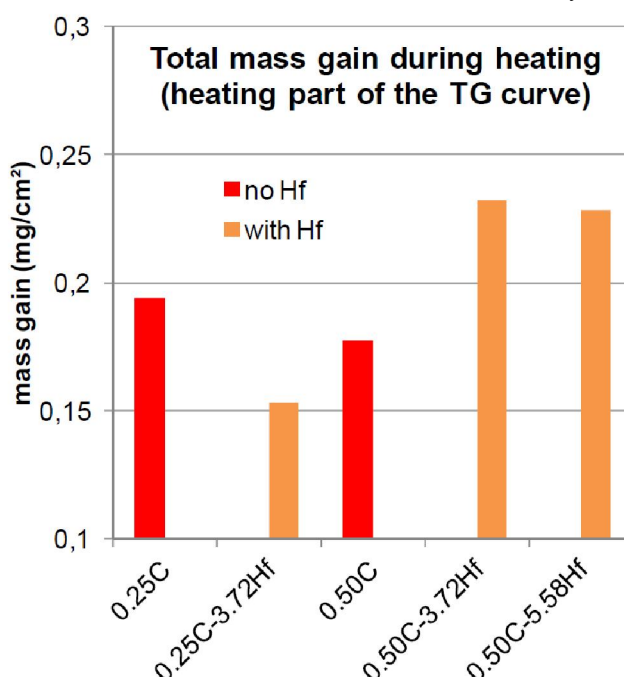


Figure 4: The total mass gain achieved during the heating, for each of the five alloys (Ni-25wt.%Cr-xC(-yHf))

As for the cobalt-based alloys previously studied the oxidation rate during heating was also characterized by calculating the value of the instantaneous linear constant for each temperature, from the data files corrected from the air buoyancy variation:

$$K_1(T_n) = [(\Delta m/S)_{n+1} - (\Delta m/S)_n] / (T_{n+1} - T_n)$$

(n : the step number, T_n : the corresponding value, $(\Delta m/S)_n$: the corresponding mass gain per cm^2).

$K_1(T)$ was plotted in the Arrhenius scheme for the two Hf-free nickel-based alloys in Figure 5 and for two of the three Hf-containing ones in Figure 6, in the temperature range defined by the temperature of oxidation start of the alloy (as earlier defined) and the stage temperature (1200°C). In all cases the obtained graphs are here too similar to straight lines. This means that, probably, phenomena are of same nature all along the heating and their kinetic obey an Arrhenius law. In the five cases a regression line was determined, and its equation was used to extract a value of activation energy, by multiplying the negative slope (coefficient of “ x ” in the regression equation) by the opposite of the perfect gas constant $R = 8.314 \text{ J mol}^{-1} \text{ K}^{-1}$.

The obtained values of activation energy are presented as a histogram in Figure 7. One can see in this figure that these ones are globally between 150 and

Full Paper

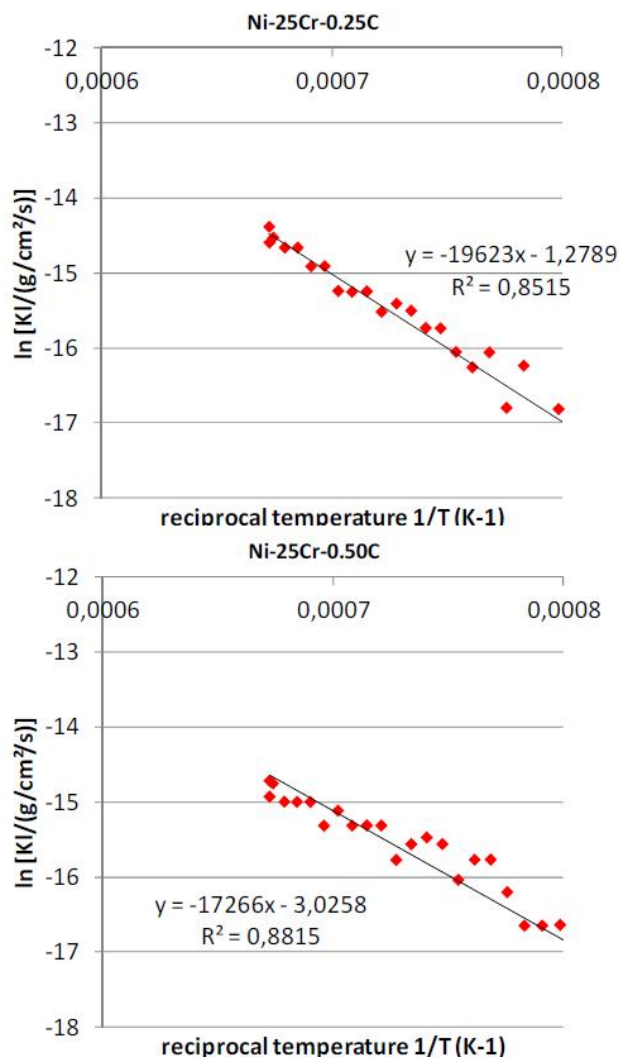


Figure 5 : Arrhenius plot of the linear constant K_1 for the two Hf-free ternary alloys

200kJ/mol but with maybe a tendency to be higher for the Hf-containing alloys than for the Hf-free ones. However, since the lowest values of activation energy were obtained for the two Hf-free alloys and for the {0.5C-3.72Hf}-containing one - these three alloys presenting as common point to contain some chromium carbides in their microstructures – one can suspect that the highest activation energy values are due to an interdendritic carbides network only composed of HfC ones.

Results: Isothermal oxidation

When more conventionally plotted (i.e. as $\Delta m/S = f(t)$) the isothermal mass gain curves of all the five alloys are globally parabolic. The total mass gains achieved during the whole isothermal stage at 1200°C were determined on these parabolic curves and the re-

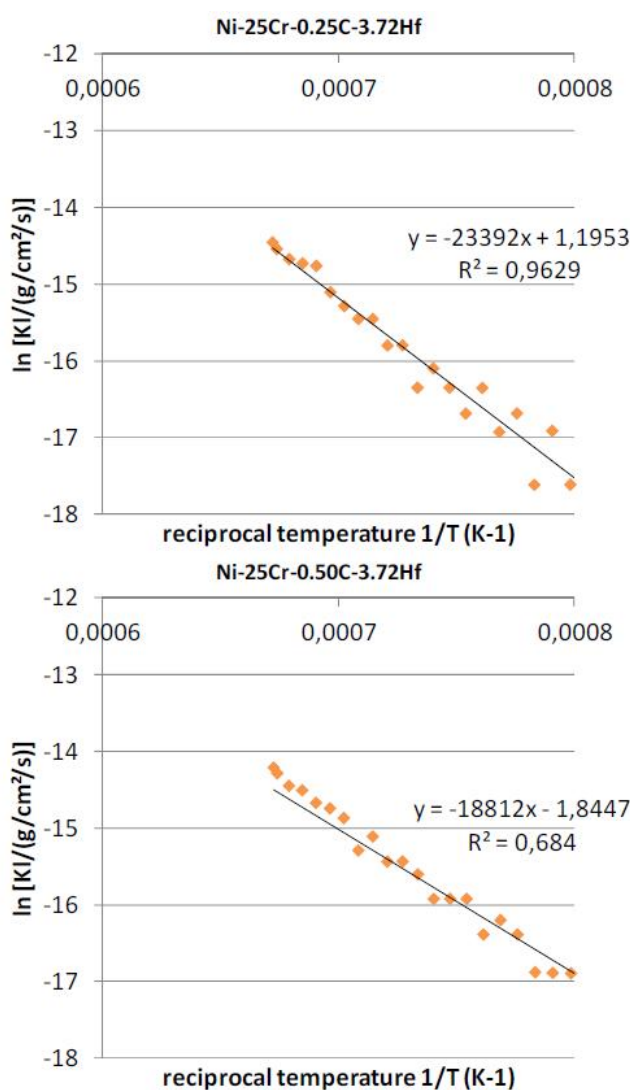


Figure 6: Arrhenius plot of the linear constant K_1 for two of the Hf-containing quaternary alloys

sults are displayed again as a histogram, presented in Figure 8. In this one it can be seen that no general rule can be revealed concerning an influence of the carbon content and an effect of the presence of hafnium. One can just notice the rather fast oxidation of the Hf-richer alloy by comparison with the four other studied alloys.

In contrast, significant differences can be highlighted between these nickel-based alloys – containing or not hafnium – and their homologous cobalt-based alloys previously studied^[8]. The isothermal mass gains are about ten times lower here, which is really significant despite the a little longer isothermal stage in the case of the cobalt-based alloys (50 hours instead 46 hours here).

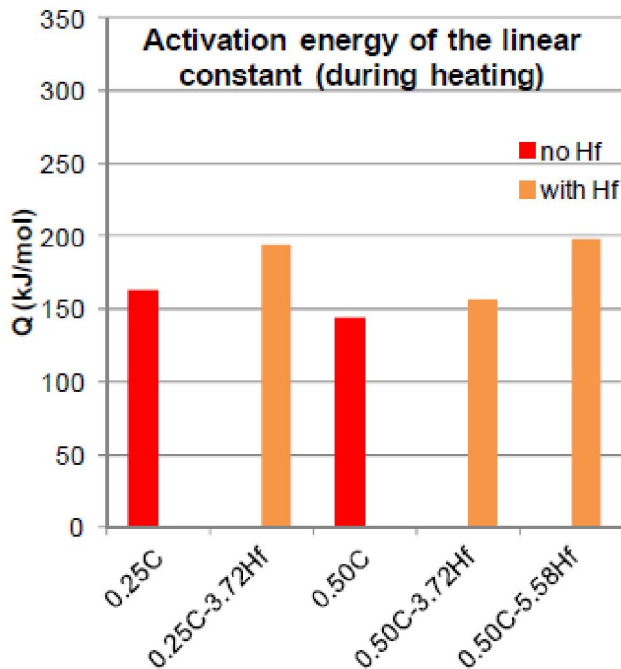


Figure 7: The activation energies for the linear constant K_1 for the five alloys oxidized during the heating

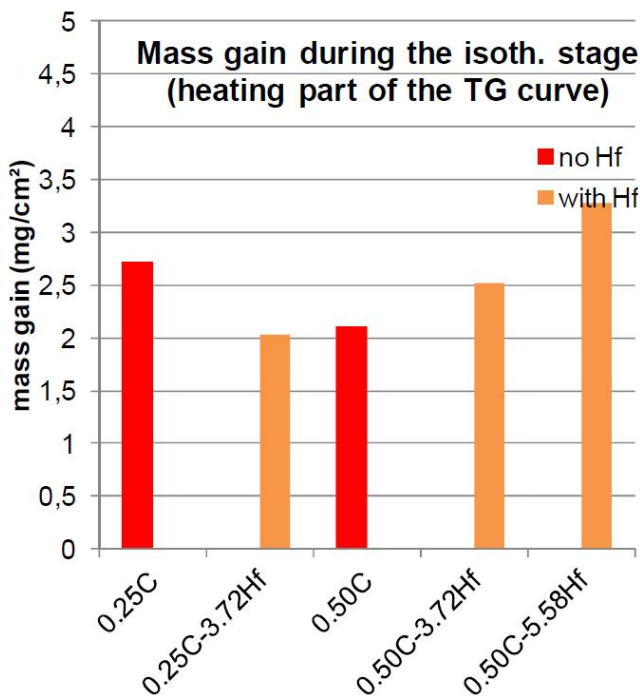


Figure 8: The total mass gain achieved during the heating for each of the five alloys (Ni-25wt.%Cr-xC(-yHf))

Results: Oxide spallation at cooling

During the cooling following the isothermal stage, the thermal contraction occurring with different rates for on the one hand the alloy, and on the other hand the external oxide, induces compressive stresses for the

external oxide. If a part of this stress state is compensated by creep deformation of the oxide in the first part of cooling (when the temperature is still high enough to allow this visco-plastic deformation), the oxide scale is after more and more threatened by spallation, a phenomenon inducing a more or less continuous mass loss which can be detected by the thermobalance. The temperatures of spallation start were determined on the cooling parts of the $\Delta m/S = f(T)$ curves, for the five alloys. The results are presented as a histogram again, in Figure 9. There is a great difference between the Ni-Cr-C alloys on the one hand, and the Ni-Cr-C-Hf ones on the other hand, illustrated by the two $\Delta m/S = f(T)$ curves given above in Figure 2 for the two 0.25C-containing alloys without and with Hf. Indeed, the temperatures at which spallation occurred during the cooling phase of the thermogravimetry tests are much lower in presence of hafnium in the alloy, more than 250°C lower for the 0.25C-containing alloys and 300°C and more for the 0.50C-containing ones. Furthermore, the effect of spallation start temperature lowering is stronger for a higher Hf content (more than 400°C lower for the Ni-25Cr-0.50C-5.58Hf alloy than for the Ni-25Cr-0.50C one). In addition the spallation is also delayed of 100-150°C to lower temperatures by comparison

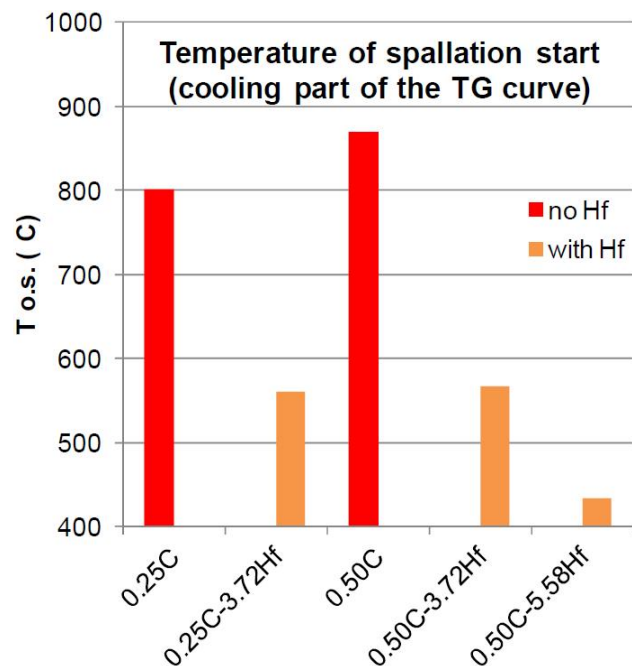


Figure 9: Temperatures at which the external oxide begins to encounter spallation during the cooling, for each of the five alloys (Ni-25wt.%Cr-xC(-yHf))

Full Paper

to the Hf-containing cobalt-based alloys^[8] (for which Hf had already a beneficial effect on the oxide spallation resistance). This led also to a loss of oxide, and then a mass fall, which is globally more important for the Hf-free nickel-based alloys than for the Hf-containing ones (Figure 10). The well-known benefit of hafnium for the external oxide scale adherence is then observed here, while the opposite effect was curiously observed in the case of the cobalt-based alloys^[8]. In this later case this was explained by the high mass gain achieved isothermally at 1200°C (especially for the Hf-containing cobalt alloys) which did not allow maintain so easily the scales during the cooling, with additionally a much greater mass of oxide to lose.

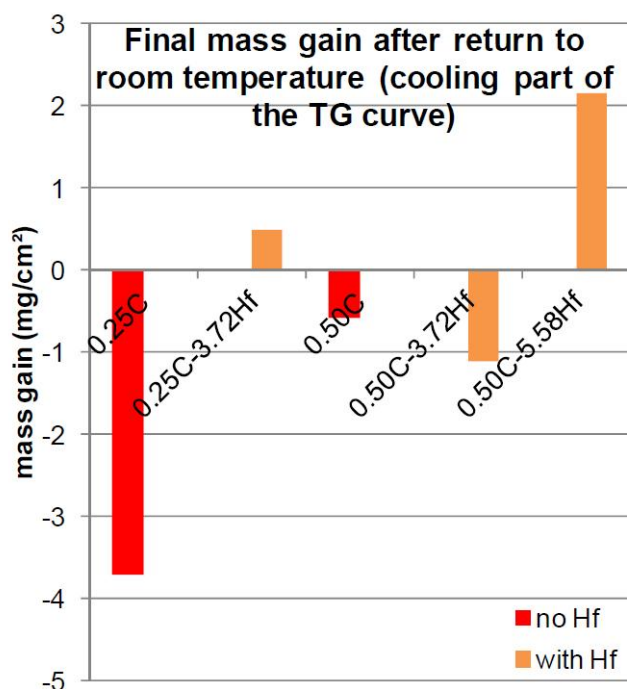


Figure 10 : The final mass gain remaining after complete cooling, for each of the five alloys (Ni-25wt.%Cr-xC(-yHf))

General commentaries

If it is well known that hafnium considerably influences how refractory alloys and superalloys behave in oxidation at high temperature when present in rather small quantities, the changes in behavior in this field for high contents as tested in this work are not known. In the present study, 3.72wt.% and 5.58wt.% of Hf were added to model chromium-rich nickel-based alloys containing two different amounts in carbon, which allowed to develop significant interdendritic networks of hafnium carbides known to be especially stable at high

temperature, with additional chromium carbides for one of the three Hf-containing alloys. The kinetic of oxidation was here specified by thermogravimetry for the three parts of a conventional oxidation test – heating, isothermal stage and cooling – leading to results to be compared with the similar ones obtained for ternary Ni-Cr-C alloys with the same Cr and C contents. As previously encountered for cobalt-based alloys the mass gain induced by oxidation during the heating phase was here detected for temperatures lower than for the Hf-free alloys. But contrarily to what was seen for the cobalt alloys the total mass gain during heating tended to be here higher in presence of Hf in the alloys. During the same heating phase the instantaneous linear constant was dependent on temperature according to an Arrhenius law in all cases (as the cobalt-based alloys) and the corresponding activation energies seemingly depend on the C and Hf contents less than for the cobalt alloys. The dependence on the alloy chemical composition of the mass gain achieved during the whole isothermal stage was also less pronounced than for the cobalt alloys. This is especially concerning the mass variations during cooling that there were more differences between the Hf-free nickel-based alloys and the Hf-containing ones: an oxide spallation delayed down to lower temperature (already seen for the cobalt alloys), and, after return to room temperature, a mass loss less important in presence of hafnium by comparison with the ternary alloys (this was in contrast the contrary for the cobalt-alloys).

CONCLUSIONS

Here too the comparative study of the behaviors in oxidation at high temperature of alloys containing hafnium carbides and of other ones in which only chromium carbides are present led to interesting comparisons, for the heating and cooling phases as well as for the isothermal stage. The noticed differences induced by the presence of hafnium or not were not always the same as the ones previously revealed for cobalt-based alloys. But this was explained by the great differences of mass gains between the two families of alloys, cobalt-based and nickel-based at this so high temperature. As this was previously done for the cobalt-based alloys without or with Hf, the present kinetic results and

their variation with the presence of hafnium^[11] will be more deeply studied and commented by examining the surface and sub-surfaces states of the oxidized samples. The presentation of these metallographic results and their exploitations to complete the analyses will be done in the second part of this work^[12].

REFERENCES

- [1] M.J.Donachie, S.J.Donachie; Superalloys: A Technical Guide (2nd Edition), ASM International, Materials Park, (2002).
- [2] M.Durand-Charre; The Microstructure of Superalloys, CRC Press, Boca Raton, (1997).
- [3] J. Young; High temperature oxidation and corrosion of metals, Elsevier, Amsterdam, (2008).
- [4] P.Kofstad; High Temperature Corrosion, Elsevier applied science, London, (1988).
- [5] S.Vasseur; Patent EP 511099.
- [6] P.Berthod, L.Aranda, C.Vébert, S.Michon; Calphad/Computer Coupling of Phase Diagrams and Thermochemistry, **28**, 159 (2004).
- [7] P.Berthod; Materials Science: An Indian Journal, **9(9)**, 359 (2013).
- [8] P.Berthod, E.Conrath; Materials Science: An Indian Journal, accepted paper.
- [9] P.Berthod; The Open Corrosion Journal, **4**, 1 (2011).
- [10] P.Berthod; The Open Corrosion Journal, **2**, 61 (2009).
- [11] P.Berthod, P.Villeger; Materials Science: An Indian Journal, accepted paper.
- [12] P.Berthod, E.Conrath; Materials Science: An Indian Journal, to be submitted.